

in December 1983, but these measurements are not yet fully reduced.

Using the calibrated (V-B)-(B-L) diagram, we determined the parameters T_{eff} and $[\text{Fe}/\text{H}]$ for each programme star (Fig. 4a). For this purpose we assumed that interstellar reddening in the South Galactic Pole field SA141 can be neglected, and we adopted a constant foreground reddening of $E(B-V)_J = 0^m.05$ for SA94. The distribution of the stars in Fig. 4a indicates that their metallicities are in the range $-1.0 \leq [\text{Fe}/\text{H}] \leq 0.0$. In the gravity-sensitive (V-B)-(L-U) diagram (Fig. 4b) the programme stars populate a narrow range suggesting that the gravities are around $\log g = 4.2 \pm 0.3$. This means that our stars are probably all dwarfs with only a few possible subgiants.

An empirical absolute magnitude calibration was derived by using the data of Cayrel de Strobel and Bentolila (1983, *Astronomy and Astrophysics* **119**, 1). From their $[\text{Fe}/\text{H}]$ catalogue we took all stars with known distances, and with the same range in T_{eff} , $[\text{Fe}/\text{H}]$ and $\log g$ as our programme stars, to construct an empirical absolute magnitude-temperature relation. With this relation we determined the distances of the programme stars in SA141 and SA94.

In Fig. 5 the metallicities are plotted as a function of vertical distance z above the plane. The z values of the programme stars observed until now vary from almost zero up to $z = 1,000$ pc with a few stars beyond this. The diagram clearly shows a correlation between distance and metallicity in the sense that stars further away from the plane are systematically metal-deficient. For example, stars at $z = 750$ pc have a mean metallicity of $[\text{Fe}/\text{H}] = -0.7$ which is five times more metal-weak than the sun.

Our calibrations are in many respects preliminary and improvements are expected for the near future. Measurements of many more nearby metal-deficient stars analysed spectroscopically are now available in the Walraven system so that the calibration of the (V-B)-(B-L) diagram can be put on a broader observational basis. Furthermore, for the determination of the absolute magnitudes we disregarded such effects as metallicity or age differences between the stars and used a mean $M_V - T_{\text{eff}}$ relation. A more detailed procedure is clearly needed.

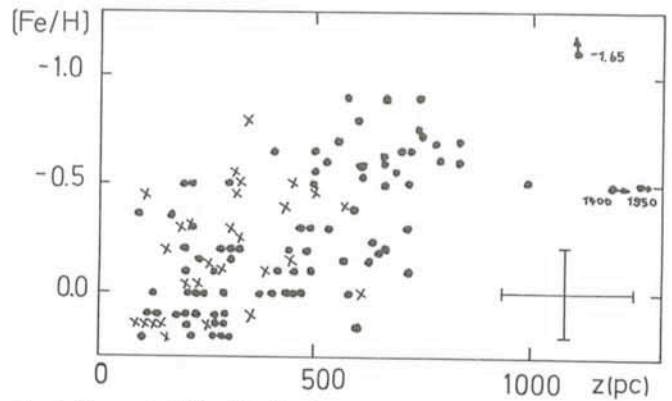


Fig. 5: The metallicities $[\text{Fe}/\text{H}]$ of our programme stars as a function of vertical distance z above the galactic plane. The diagram clearly shows that the metal content of the stars decreases rapidly as we go away from the disk into the halo.

Nevertheless, our preliminary results are in reasonable agreement with previous determinations of abundances in the direction of the galactic poles. The earlier work by Blaauw and collaborators indicated that the metallicity drops to about $[\text{Fe}/\text{H}] = -0.5$ at $z = 500$ pc which compares well with $[\text{Fe}/\text{H}] = -0.4$ estimated from our Fig. 5. Our results are also consistent with the metallicities of halo stars derived from the photographic RGU colours (Trefzger, 1981, *Astronomy and Astrophysics* **95**, 184). Our data can be used to check the predicted metallicity distributions at different z heights derived by Sandage (1981, *Astronomical Journal* **86**, 1643) from the W velocity components of nearby subdwarfs and several kinematic models.

We hope to get our photometry complete in both fields down to the limiting magnitude of the telescope ($V = 14^m.7$). In SA141 this limit has been reached already, but more observations are needed in SA94. Eventually we will try to extend the observations to other fields as well.

One-mm Observations of BL Lacertae Objects

H. Steppe, Max-Planck-Institut für Radioastronomie, Bonn

Introduction

Forty years have elapsed since C.K. Seyfert in 1943 observed galaxies with strong activity in their centres. Twenty years later a new class of extragalactic objects entered the scene: the quasi-stellar objects (QSOs or quasars) representing the most extreme examples of energy output in the Universe. Today there is growing evidence for a continuity of properties among these "active galactic nuclei" (AGN) and it is now generally agreed that what is happening in the centres of these objects is qualitatively the same. This large group of objects also includes other active galaxies, namely radio galaxies with strong emission lines and *BL Lacertae objects*. The latter are named after their prototype lying in the constellation Lacertae (the lizard) and are abbreviated as BL Lac objects. The aim of this article is to describe and interpret some results obtained from 1-mm observations of these BL Lac objects.

Observations in this part of the spectrum are challenging. The Earth's atmosphere is almost opaque to much of the radiation, mainly due to the water vapour content of the atmosphere. To overcome this difficulty observations must be carried out on high, dry mountain sites. In the absence of suitable radio telescopes (surface accuracies of $\sim 50 \mu\text{m}$ are needed), we had to use large optical telescopes, in particular the ESO 3.6 m telescope on La Silla and the 6 m SAO telescope at Zelenchukskaja in the Caucasus.

What Are BL Lacs?

The properties of BL Lacs can be summarized as follows:

- Nearly all known BL Lac objects have been discovered because they are radio sources.
- Their radio spectra ($S_\nu \propto \nu^\alpha$) are flat and often inverted, i. a. $\alpha \geq 0$.

- The radiation emanates from a compact region (~ 1 pc) of non-thermal radio emission with an extremely high brightness temperature ($T \approx 10^{11 \pm 1}$ K).
- BL Lacs show rapid variability at radio, infrared and optical wavelengths.
- They are highly polarized (up to 30%) and the polarization is strongly variable.
- In several cases BL Lac objects appear to reside in giant elliptical galaxies.

The properties of BL Lac objects and radio loud quasars overlap to a certain degree, but the principal *difference* between these two types of objects lies in a deficiency of optical emission lines in BL Lac objects.

BL Lacs lack the broad emission line regions seen in quasars which surround and partially hide the very centre of the AGNs by gas and dust. In BL Lacs we are viewing directly the central mysterious engine which is yielding prodigious amounts of power of the order of 10^{46} erg/sec over the wavelength region from the radio to X-rays. Observations of the spectral energy distribution provide crucial information on the emission mechanism operating in these sources. The continuum has now been measured at all conventionally observable wavelengths such as the radio, infrared, optical and even in some cases in the ultraviolet and X-ray wavelength bands. However, there is an irritating gap of 3 orders of magnitude in frequency between the near infrared and the high frequency radio regime. In this gap information about the spectral behaviour of celestial sources is only gathered at a very slow rate. The extension of the observations to millimetre wavelengths is especially important in order to define the spectral break which must generally occur between the radio and infrared regions. Furthermore, at millimetre wavelengths one is looking deeper into the source and sees the most compact components out of which a major proportion of the energy is emitted.

The Bolometer as the Detecting Element

For continuum measurements around 1 mm wavelengths (~ 300 GHz), bolometers are still the most sensitive type of receivers, since they can use very large bandwidths. Our bolometer, cooled with liquid ^3He down to 0.3 K, consists of a gallium-doped germanium chip as the temperature sensing element. It is—as usual at these wavelengths—of the composite type, in which the energy absorption and temperature measuring layers are separated. The large band-width of approximately 0.5 mm (~ 150 GHz) is limited by diffraction at the telescope aperture at the long wavelength side (ca. 1.5 mm). The short wavelength limit is set by a filter in combination with absorption by the water vapour in the atmosphere.

A dual-beam chopping system is used. The half-power beam diameter is about $120''$ at the 3.6 m ESO telescope and the separation of the beams is also $120''$. The signal is chopped by means of a sector mirror rotating at 10 Hz.

Flux density calibration and extinction at these wavelengths are usually determined from observations of the planets using their measured brightness temperatures.

However, since the planets cannot be observed around the clock and the conditions of the sky change in a rapid and unpredictable way, we also made "Sky dips" i.e. pointing the telescope at blank sky at different elevations and recording the thermal radiation of the atmosphere as a function of the airmass. The measurements of the transmission of the atmosphere (typically of the order of 70% to 80%) then yield the atmospheric water vapour content, which was combined with absorption line data for atmospheric water vapour and oxygen

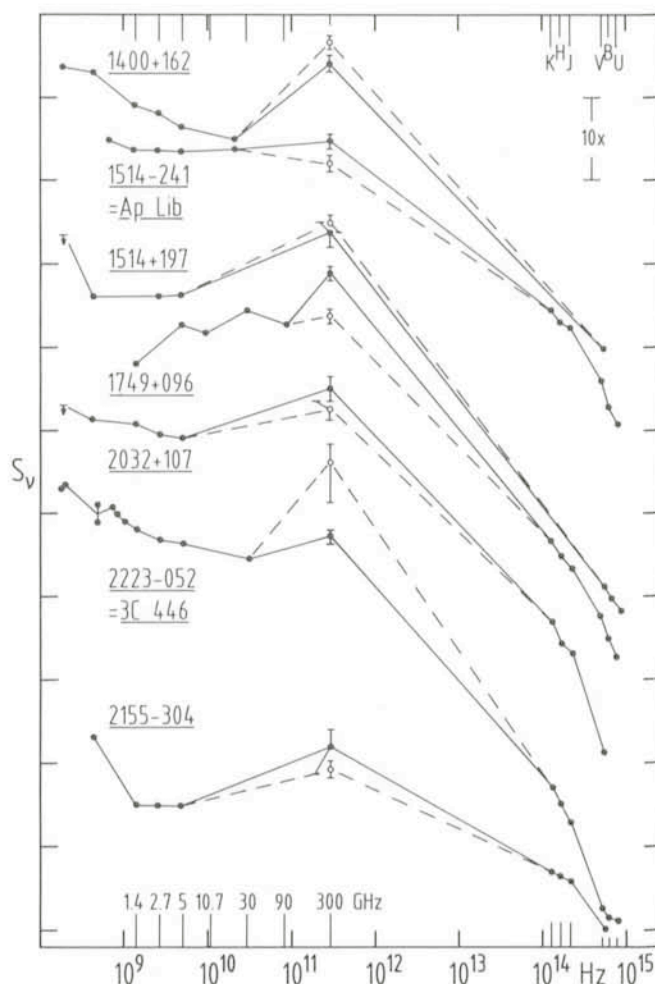


Fig. 1: Overall spectrum (from radio to optical wavelengths) of those BL Lac objects, for which 1 mm observations have been obtained at two observing sessions (● June/July 1982, ○ July 1983). The λ 1 mm flux densities are derived assuming a spectral index $\alpha = 0$. For reasons of clarity only error bars for 1 mm flux densities are given. The Optical Violent Variable (OVV) 3C446 is included in the sample; it showed an outburst at λ 1 mm during July 1983, followed by an optical outburst in August 1983 (IAU circular No. 3856).

to calculate the exact spectral response in the bandpass and the effective observing wavelength.

The Observations

With the bolometer attached to the prime focus of the ESO 3.6 m telescope on La Silla a source of 1 Jy is detected with a signal-to-noise ratio of 3 in one hour integration time. The observations were performed at two epochs, in July 1982 and in June/July 1983, both times under unfavourable weather conditions.

Our BL Lac objects were selected from the list of Hewitt and Burbidge (1980). About 20 BL Lac objects have an expected flux density at 1 mm wavelength greater than our system sensitivity limit (1 Jy) if the spectrum is extrapolated from optical/infrared and from the radio region towards 15 mm. Out of these objects 15 have been observed. Additionally, six likely BL Lac candidates, not listed in the above-mentioned quasar catalogue were chosen because of their flat radio and steep infrared spectra. The radio data were taken from the available catalogues, and the infrared data have been published by Allen, Ward and Hyland (1981).

Radio and Infrared Spectrum

Fig. 1 shows the spectral distribution for a few BL Lac objects from the radio to the infrared/optical domain. Data at 1 mm could only be obtained at both observing periods for the few sources presented in the figure. For reasons of clarity only error bars for the flux densities at 1 mm are depicted in the figure. They are estimated to be about 25 per cent, mainly due to uncertainty in calibration.

Most BL Lacs show inverted (65 %) or flat (35 %) radio spectra so that the flux at 1 mm often exceeds the value at lower frequencies. The spectrum of radio quasars on the other hand is flat or decreasing with frequency.

Based on their spectra at high radio frequencies, BL Lac objects will be very numerous in future mm surveys and become the most common type of objects. Extrapolation of the high-frequency radio spectrum towards 1 mm gives a close correlation between the observed and extrapolated fluxes at 1 mm.

The ratio in flux density of the near infrared (NIR) to the mm range S_{IR}/S_{mm} is a few times 10^{-3} . Fig. 2 shows a graph of the spectral index in the near infrared (J to K, ~ 1.2 to $2.2 \mu\text{m}$) versus the spectral index between the K band and 1 mm. Though there is a wide spread in both spectral indices for a single object, a unique spectral index from 1 mm all the way to the NIR is compatible with the observations (dashed line in Fig. 2). The scatter in the diagram could be attributed partly to the variability of the sources because the observations made in the different wavebands were carried out at different epochs. This could be especially true for AO 0235+164 (e.g. strong outburst at the end of 1977). A scatter could also be caused by a misidentification of an object: 0406+121 is classified as a probable BL Lac object (Aaronson and Boronson, 1980).

Radiation Processes in BL Lacs

A uniform spectral slope from 1 mm to the NIR can most easily be explained if a single radiation mechanism is the origin of both the radio and infrared emission. The simplest mechanism is the *synchrotron radiation process*. It would also explain variability and strong polarization. The variability increases with frequency so that at millimetre wavelengths variations on a time scale of days are observed. As an example we list in the table our measurement of the source 1749+096:

Source	Date of Observation	$S_{1\text{mm}}$ (Jy) assuming $\alpha = 0$
1749+096	07.07.1982	4.4
	08.07.1982	8.5
	09.07.1982	3.2
	10.07.1982	7.2

Unfortunately we have not yet undertaken polarization measurements, but for the next observing run our instrument will be equipped with a simple polarimeter.

For an explanation of the overall spectrum of the BL Lacs from radio to X-rays the synchrotron-self Compton (SSC) theory seems to be favoured by most astronomers. In the SSC mechanism the synchrotron radiation is scattered by the relativistic electrons to higher energies. This would explain why X-ray emission has been observed for nearly all AGNs which are chosen from radio surveys. The flat or inverted part of the radio spectrum in BL Lac objects could be composed of several distinct, compact components which show synchrotron-self absorption at different wavelengths. The observed turnover frequency due to the synchrotron-self absorption

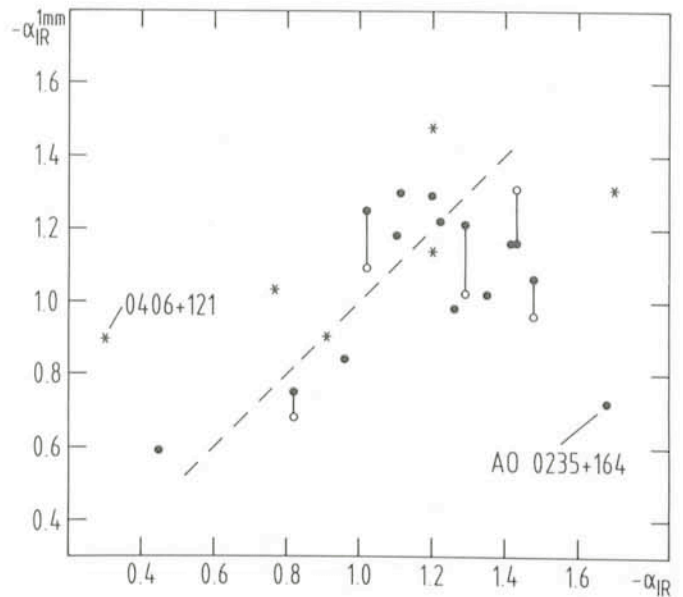


Fig. 2: Correlation between the spectral index in the near infrared (α_{IR}) and the spectral index derived from the flux at 1 mm and that in the K-band at $2.2 \mu\text{m}$ ($\alpha_{IR}^{1\text{mm}}$). Filled circles represent confirmed BL Lac objects while probable BL Lacs are shown by asterisks. Filled circles are from observations in June/July 1982, while open circles belong to July 1983 measurements.

cutoff allows an estimate of the angular diameter which turns out to be a few 10^{-6} arcsec. These most compact regions are the places where the X-ray photons are created by the inverse Compton effect and which make up the highest frequency part of the spectrum in BL Lac objects. At frequencies higher than the turnover frequency the spectrum becomes optically thin and can be represented as a power law $S_\nu \propto \nu^\alpha$, with a single spectral index extending into the UV region.

Future Prospects

Surveys at 1 mm should provide BL Lacs as the most common type of objects. Because the typical variability time scale is of the order of days, it is essential that simultaneous observations at mm and shorter wavelengths are performed, both for measuring the total intensity—to determine the true spectral behaviour—and also the polarization. A systematic monitoring of BL Lac objects in the mm waveband yields opportunities for probing the shortest timescales of these sources. And finally, future millimetre Very Long Baseline Interferometry (VLBI) observations could ultimately reveal the innermost engine on scales of ~ 10 mpc, determine its shape and so provide insight into the origin of activity in BL Lac objects. It is obvious that these problems require a lot of telescope time in long-term programmes. Thus, we are looking forward to using a telescope especially built for mm observations on Pico Veleta, a 2,850 m high mountain near Granada (Spain), hopefully in 1984.

References

- Aaronson, M., Boronson, R.: 1980, *Nature* **283**, 746.
 Allen, D. A., Ward, M. J., Hyland, A. R.: 1982, *Monthly Notices of the Royal Astronomical Society* **199**, 969.
 Hewitt, A., Burbidge, G.: 1980, *Astrophysical Journal Suppl.* **43**, 57. IAU circular No. 3856 (1983).